AFRL-AFOSR-UK-TR-2018-0027

Mode-locked Diode Lasers from Microscopic Analysis to Femtosecond Pulses

Martin Hofmann
RUHR-UNIVERSITAT BOCHUM

02/28/2018
Final Report

Air Force Research Laboratory
AF Office Of Scientific Research (AFOSR)/ IOE
Arlington, Virginia 22203
Air Force Materiel Command

REPORT DOCUMENTATION PAGE

Form Approved
OMB No. 0704-0188

1. REPORT DATE *(DD-MM-YYYY)*	2. REPORT TYPE	3. DATES COVERED *(From - To)*
02-08-2018	Final	15 Jul 2014 to 14 Jul 2017

4. TITLE AND SUBTITLE
Mode-locked Diode Lasers from Microscopic Analysis to Femtosecond Pulses

5a. CONTRACT NUMBER

5b. GRANT NUMBER
FA9550-14-1-0137

5c. PROGRAM ELEMENT NUMBER
61102F

6. AUTHOR(S)
Martin Hofmann

5d. PROJECT NUMBER

5e. TASK NUMBER

5f. WORK UNIT NUMBER

7. PERFORMING ORGANIZATION NAME(S) AND ADDRESS(ES)
RUHR-UNIVERSITAT BOCHUM
UNIVERSITTSSTR. 150
BOCHUM, 44801 DE

8. PERFORMING ORGANIZATION REPORT NUMBER

9. SPONSORING/MONITORING AGENCY NAME(S) AND ADDRESS(ES)
EOARD
Unit 4515
APO AE 09421-4515

10. SPONSOR/MONITOR'S ACRONYM(S)
AFRL/AFOSR IOE

11. SPONSOR/MONITOR'S REPORT NUMBER(S)
AFRL-AFOSR-UK-TR-2018-0027

12. DISTRIBUTION/AVAILABILITY STATEMENT
A DISTRIBUTION UNLIMITED: PB Public Release

13. SUPPLEMENTARY NOTES

14. ABSTRACT
Grant finished and final report submitted. The goal of the project was to elaborate how sub-100 fs optical pulses can be generated with mode-locked semiconductor diode lasers. Our strategy for this elaboration is based on a fundamental understanding of the pulse shaping dynamics in the semiconductor with particular emphasis on the influence of many-body effects and nonequilibrium dynamics in the semiconductor.

15. SUBJECT TERMS
Semiconductor Lasers, maxwell bloch equations, modelling dpssl, many body modelling of lasers, EOARD

16. SECURITY CLASSIFICATION OF:			17. LIMITATION OF ABSTRACT	18. NUMBER OF PAGES	19a. NAME OF RESPONSIBLE PERSON
a. REPORT	b. ABSTRACT	c. THIS PAGE			LOCKWOOD, NATHANIEL
Unclassified	Unclassified	Unclassified	SAR		19b. TELEPHONE NUMBER *(Include area code)* 011-44-1895-616005

Standard Form 298 (Rev. 8/98)
Prescribed by ANSI Std. Z39.18

August 2018

Grant Award No. FA9550-14-1-0137

Mode-locked Diode Lasers from Microscopic Analysis to Femtosecond Pulses

R. Pilny, B. Döpke, C. Brenner, and M.R. Hofmann

Photonics and Terahertz technology, Ruhr University Bochum, Germany

The goal of the project was to elaborate how sub-100 fs optical pulses can be generated with mode-locked semiconductor diode lasers. Our strategy for this elaboration is based on a fundamental understanding of the pulse shaping dynamics in the semiconductor with particular emphasis on the influence of many-body effects and nonequilibrium dynamics in the semiconductor.

Semiconductor diode lasers are extremely efficient, compact and cost effective. In addition, semiconductor lasers provide a broad material gain spectrum. Therefore they should be suited well for extremely compact femtosecond light sources. Given the pure width of the material gain spectrum, pulse widths below 50 fs should be achievable. However, this enormous potential has not yet been explored by far. Therefore, our aim in this project is to clarify the problems of challenges in ultrashort pulse generation with diode laser and to develop a strategy how to create sub-100 fs pulses with such devices.

Our strategy was to compare our experimental results to a sophisticated theoretical approach. In the first approach, we first used the phenomenological travelling wave model developed by Javaloyes et al. [1,2], and planned to replace the simple susceptibility in the model by data from a look-up table generated with a microscopic many-body model. For that purpose, we received susceptibility data for our laser structure generated by Profs. Joerg Hader, Jerry Moloney and Stephan Koch (Univ. of Arizona).

1. Modelling results

We implemented the phenomenological model by Javaloyes and simulated pulse generation with it. However, while some simplifications of the model hold true for some semiconductor lasers, it has turned out to be not suited for our laser systems.

The model assumes that the pulses are rather short (in the regime of a few hundred femtoseconds), while the actual pulses emitted by our devices are in the range of picoseconds due to the strong chirp. This means that the carrier density change of a spatial simulation point cannot be neglected when the pulse is propagating through it. Furthermore, the pulse collision is implemented only with a factor in intensity, which holds not true for our devices. Thus, the pulses provided by the model are too short. Moreover, they are always symmetric in shape (see example shown in Fig.1) which is in clear contrast to the pulses emitted by our devices. The pulses emitted in experiment are strongly chirped (see example shown in Fig.2) and asymmetric in time. Accordingly, the most important effects for the pulse shaping and its improvement are

obviously not captured in the model. That means, that the model by Javaloyes, in contrast to our initial strategy, is not suited for this project.

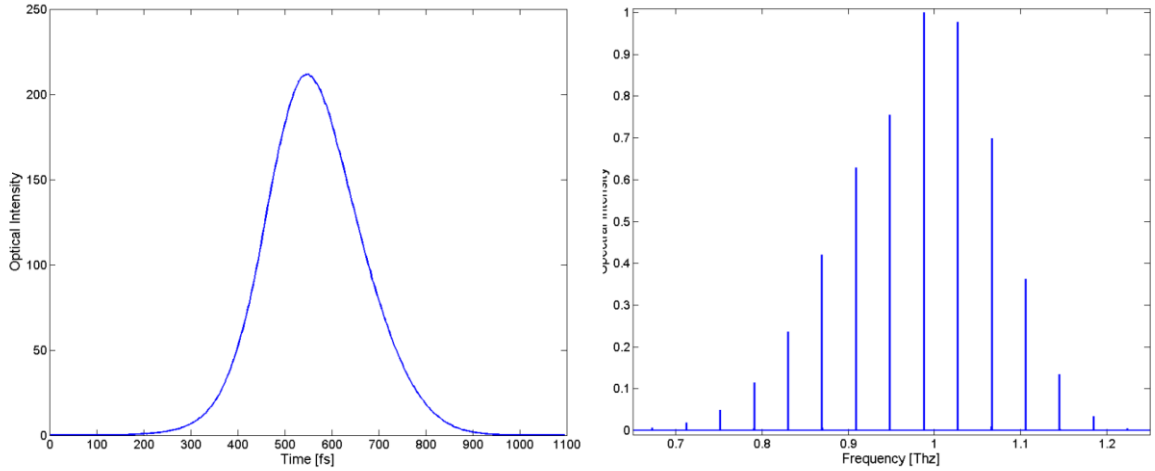

Fig.1: An exemplary pulse and the corresponding spectrum simulated by the Javaloyes and Balle model [1,2]. Though the spectrum is slightly asymmetric in shape, the emitted pulses are nearly symmetric and exhibit a dominant Gaussian shape.

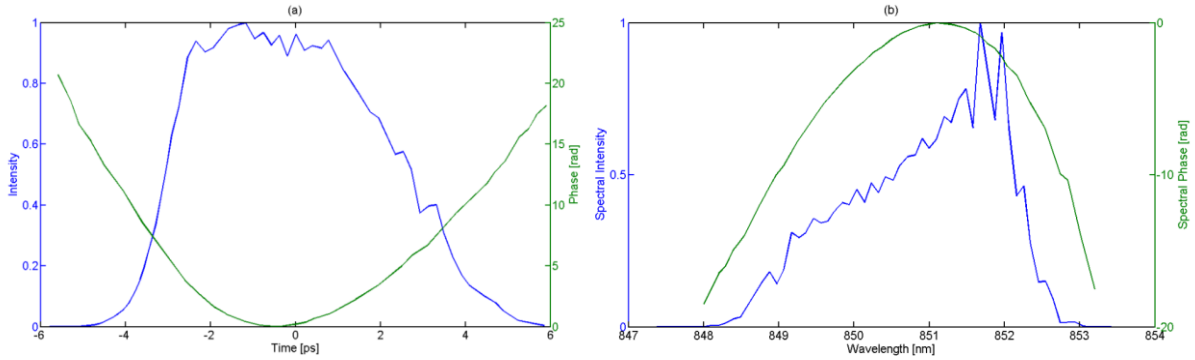

Fig. 2: Measured Frog Trace (left) and emission spectrum (right) of an actually emitted pulses by our device. The pulse is strongly linearly chirped and strongly asymmetrical, the spectrum is also asymmetrical.

Consequently, we had to change our approach by implementing a new model. In the second step, we selected the well-established Haus master model [3]. In the model, we implemented a ring oscillator to avoid the complication of pulse collision. In addition we assumed the length of the oscillator to be sufficiently large in order to have relaxed gain and absorption. Figure 3 shows the scheme of the complete Haus master model, which is based on the Haus master equation. The electric field the Haus master equation can be reduced to two equations:

$$-j\psi + g - l - jx + \frac{(1+j\beta)^2}{\tau^2}\left(\frac{g}{\Omega_g^2} + jD\right) = 0$$

$$\frac{1}{\tau^2}\left(\frac{g}{\Omega_g^2} + jD\right)(2 + 3j\beta - \beta^2) = (\gamma - j\delta)A^2$$

where A is the amplitude of the pulse, g is the gain, l the linear loss, $-j\psi$ and jx are the phase shifts due to gain and loss, β the chirp, τ the pulse width, Ω_g, D the magnitude of Dispersion, γ the inversely proportional to the saturation intensity and δ effective cross section of the mode.

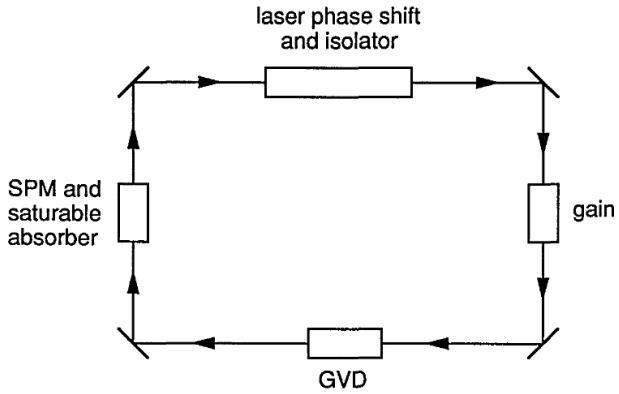

Fig 3: The Haus master model is implemented here as a ring cavity with gain, gain dispersion, self-phase modulation and group velocity dispersion, saturable absorption, as well as linear loss and phase shift [3]

Implementing this method we were able to observe the effect of gain saturation and absorber relaxation on the shape of the pulse which was not achieved with the Javaloyes model but turns out to be most important in the first attempt for comparison with experiment. Furthermore we implemented a carrier density in the semiconductor which is changing while the pulse is traveling through it. Exemplary simulation data is plotted in figure 4.

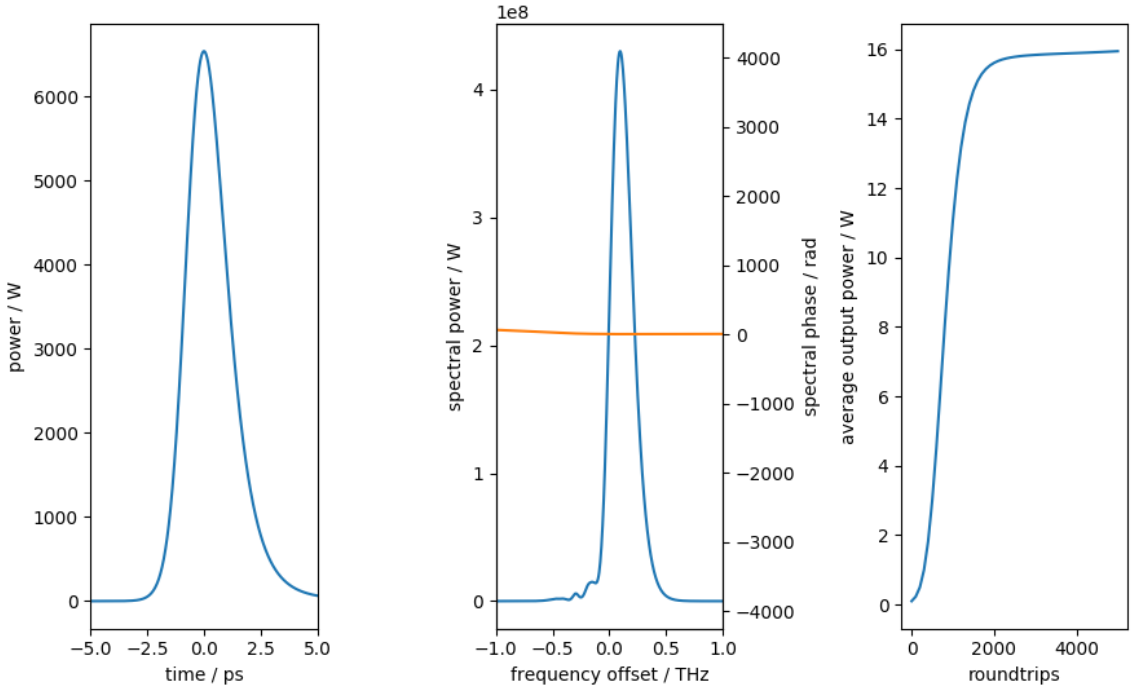

Fig. 4: Left: temporal pulse shape after 500 roundtrips. Middle: spectrum and phase retardation (red line) of the pulse. Right: evolution of the power. The simulation was initialized with noise.

Figure 4 shows the properties of the pulse generated after the 5000th roundtrip when the output has stabilized to a stable pulse train. It shows the temporal shape of the pulses which is in the range of picoseconds and is obviously shaped by the saturation effects of the gain and absorption. The graph in the middle shows the spectrum of the pulse and its spectral phase. Finally, the right part of Fig.4 shows the evolution of the power over the roundtrips indicating a steady state after ~2000 roundtrips. Though the model contains many assumptions and simplifications, it provides a reasonable qualitative agreement with our experimental observations.

To check the most important effects on the pulse generation, we varied the saturation of gain and absorption, the group delay dispersion and the width of the effective gain spectrum. In contrast to the other parameters, a variation of the width of the gain spectrum turned out to be of negligible influence on the pulse shape and the spectral shape. Thus, it can be expected that simply replacing the very easy gain spectrum of the original model by a calculated microscopic many-body gain would at the current state not provide more insight into the limiting factors for generating shorter pulses.

Nevertheless, in the next step we implemented the microscopic many-body model of the susceptibility. This was done by implementing look-up tables of the microscopic susceptibility for various carrier density into our model. These look-up-tables were calculated and provided by our partners (Prof. J. Harder) at the University of Arizona. The propagation had to be expanded in order to propagate “pulse-spectrograms” with a time-frequency distribution instead of a singular temporal pulse and its spectrum. This enables a correct representation of the chirped pulses, depicting the time at which each spectral component is present. To describe the carrier dynamics sufficiently and to be able to resolve 100 fs pulses as well as 10 ps pulses, a temporal resolution of 12.5 fs was chosen. This resulted in a spectral bandwidth of 80 THz. The frequency resolution was set to 5 GHz, which accumulates to a temporal window of 200 ps.

However, this implementation drastically increases the computational effort. It increased the calculation time for 1000 roundtrips from 2 minutes up to more than a day. To reduce the computational effort, points in time with low spectral intensity were neglected. This reduced to the simulation time for one run to less than a day. However, the search for the most suitable parameters in the model to describe the experimental results requires numerous runs to optimize these parameters. This procedure turned out not to be feasible anymore within the remaining time of the project. Due to this and due to the expectation, that the conclusions drawn from the microscopic many-body description would not help in the next optimization step, we decided to concentrate on our experimental approaches for the remaining time of the project. The microscopic description may help at a later stage when the gain and absorber saturation is optimized provided that the numerical effort can be cleverly reduced.

Thus, at the current stage, we assume that the propagation effects of the pulse through the material and the saturation dynamics of gain and absorption are more critical than the correct description of the gain shape. We experimentally analyzed the gain and absorption spectra in our system and compared the data with the spectral distribution of the emitted pulses. This is visualized in Fig.5.

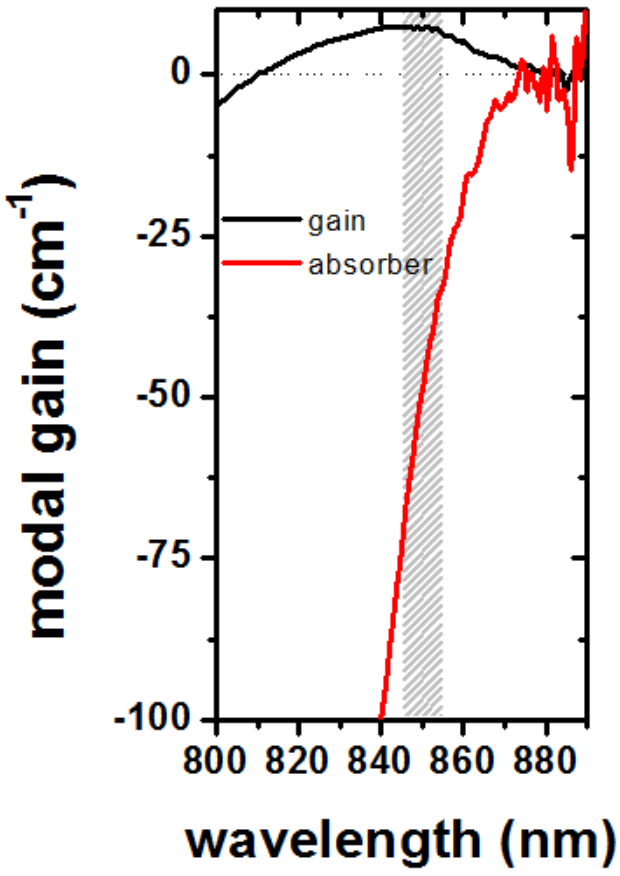

Fig. 5: Measured gain and absorption spectra of our active medium. Gain and absorption spectra were determined by transmission experiments on sections operated with forward current (gain) and reverse bias (absorption), respectively. The grey shaded area is the typical spectral range of the emitted pulses in passively modelocked operation.

From Fig. 5 it is obvious that the steep absorption edge of the absorber cuts away a major part of the available net gain spectrum. Thus, a major improvement in terms of shorter pulses can only be expected when this problem is properly attached. This aspect will be further discussed after the description of our experimental work which follows in the next section.

2. Experimental Characterization

In addition to the extensive numerical investigations, detailed experimental characterizations of a mode-locked diode laser were performed. For that purpose, we use a diode laser coupled to an external cavity laser. The external cavity enables intracavity loss and dispersion management which has turned out to be important for optimization. The optimization strategy in general is to generate strongly chirped pulses with maximum spectral bandwidth and to compress these chirped pulses externally with a pulse compressor. The direct generation of femtosecond pulses out of a diode laser is complicated by ultrafast gain saturation and thus not favorable.

For our studies, we use a multiple quantum well diode laser in an external cavity. The diode consisted of two segments, one with a length of 100 µm and the other with a length of 900 µm. Thus it was possible to explore different mode-locking regimes of the diode: passive, hybrid and active mode-locking, which will be elaborated later on.

The utilized external cavity was a FTECAL-geometry [16]. In contrast to prior research, we introduced a spatial light modulator into the cavity, which allowed us to control the spectral amplitude in addition to the dispersion of the cavity [4]. The light is coupled out of the diode onto a reflective optical grating. The dispersed light is then focused by the lens on different positions along the spatial light modulator, depending on the dispersion angle. Due to the strong chirp of the emitted pulses, an external pulse compressor was employed. By compressing the optical pulses, complete mode-locking could be verified as well as the generation of bandwidth limited pulses after compression. The complete setup is depicted in Fig. 6 [4].

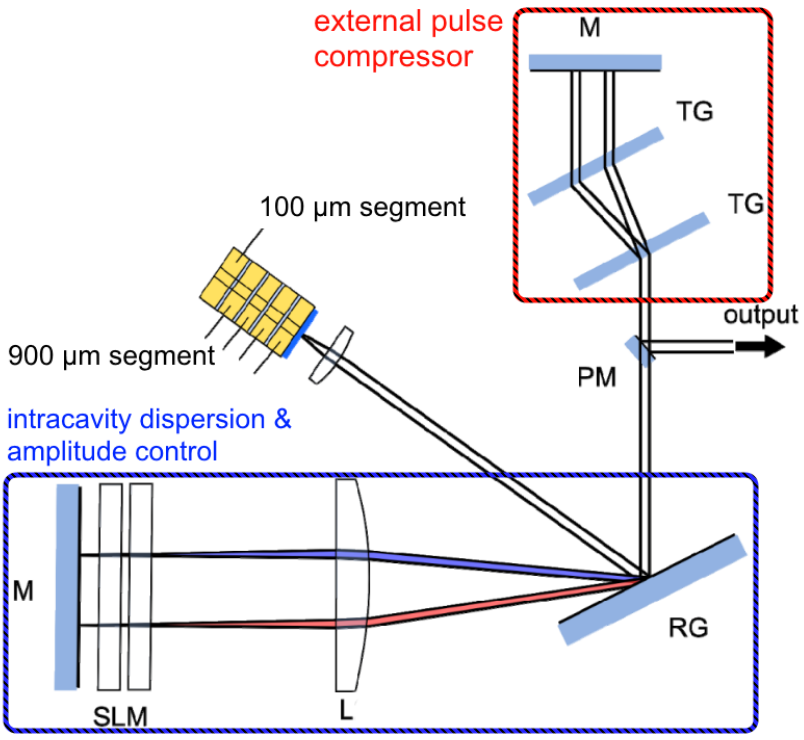

Fig. 6 Setup of an external cavity setup capable to control the dispersion of the system as well as the spectral amplitude. The 0th order of the grating was coupled into an external compression to investigate the temporal pulses.

The most common way to achieve complete mode-locking and ultrashort optical pulses is passive mode-locking. For passive mode-locking a nonlinear element is necessary. In this case a saturable absorber was realized by applying a negative bias voltage to the 100 µm segment. The 900 µm segment was used as the gain section. For optimal performance the laser was operated slightly above threshold. This provided a stable pulse train at the fundamental repetition rate of the system. For this operation point the dispersion and amplitude filters were optimized. However to optimize the dispersion and spectral amplitude systematically proved to be too time consuming and thus a non-practical approach. Consequently another strategy was performed by implemented an

evolutionary algorithm, realizing a self-optimizing laser system [4]. However, due to the strongly chirped pulses of the laser system the algorithm could not be utilized to optimize towards short temporal pulses. Instead the goal of the algorithm was set to optimize the optical bandwidth of the system. By Fourier-Transformation, a large optical bandwidth leads to a very short optical pulse width, given that the complete optical spectrum is mode-locked. Fig. 7 depicts the results of this optimization for passive mode-locking.[5-8]

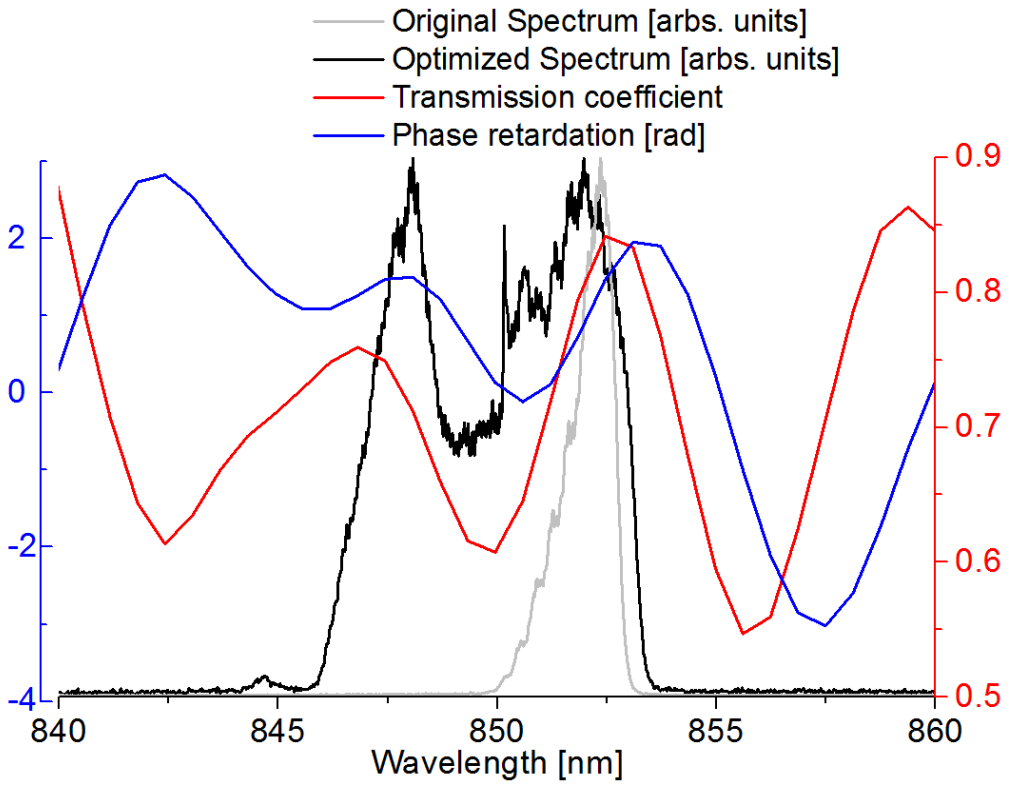

Fig. 7 shows the spectrum for passive mode-locking before optimization (light grey) and after optimization (black). Additionally the shapes of amplitude filter (red) and the dispersion (blue) are shown.

As the figure illustrates, the original optical bandwidth, which featured a spectral range of 2.34 nm, could be increased to a bandwidth of 7.2 nm. The shape of the spectrum also changed. While the original spectrum had a sawtooth shape, the optimized spectrum exhibits a more rectangular shape with a drop close to the center of the spectrum. Furthermore it is observable that the biggest increase of the optical bandwidth is due to the expansion to lower wavelengths. The optimized amplitude filter induces the highest losses to the center wavelength of the spectrum. The dispersion features a quadratic phase retardation from 848 nm to 854 nm. However, for lower wavelength the shape of the phase has higher order contributions.

In the second step, hybrid mode-locking was investigated [9-15]. For the operation point, the same parameters which were used for passive mode-locking were retained, with the exception of adding a modulation frequency. The modulation was applied to the 900 µm gain segment and featured a frequency according to the round trip time of

the external cavity. The characteristics of this mode-locking regime are shown in Fig. 8.

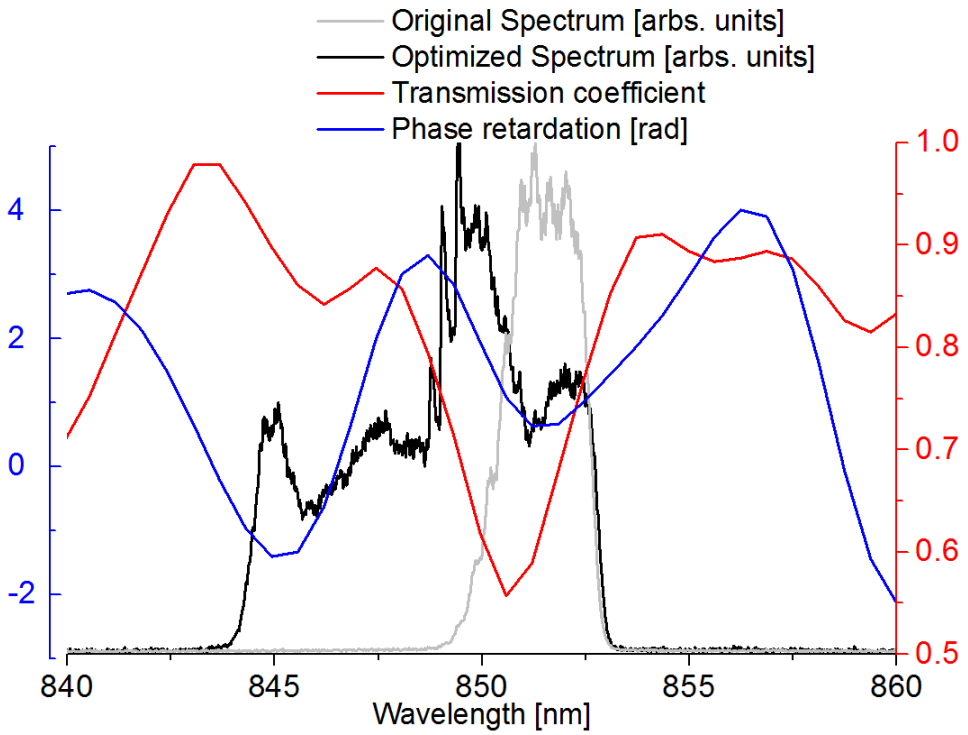

Fig. 8 shows the spectrum for hybrid mode-locking before optimization (light grey) and after optimization (black). Additionally the amplitude filter (red) and the dispersion (blue) are shown.

While the original spectrum is centered on the same wavelength as the spectrum for passive mode-locking, it has a slightly larger optical bandwidth of 3.21 nm. This bandwidth could be expanded to 8.7 nm by the optimization algorithm. The increase in bandwidth is also attributed to an addition of shorter wavelength components, but more than for passive mode-locking. The shape of the optimized spectrum is also shifted to a more rectangular appearance, however, instead of featuring a drop at 850 nm, there is a peak in the spectrum at 850 nm. Moreover, the highest losses are induced for 851 nm and decrease from 851 nm on. The phase retardation applied is highly non-quadratic and complex.

The final characterization of mode-locking regimes was done for active mode-locking. Therefore a forward current was applied to both segments of the laser diode. The current was adjusted to be slightly below the CW-lasing threshold of the system. Then the 900 µm segment was modulated with a frequency corresponding the roundtrip time of the cavity. The results of this experiment are shown in Fig. 9.

Several difference for this regime can be observed compared to passive and hybrid mode-locking. First of all, due to the absence of an absorber, the initial spectrum is blue-shifted and features a quite narrow spectral range of 0.26 nm. The range could be raised to 5.06 nm by optimization. However, opposite to the other regimes, the spectrum expanded evenly in the spectral range, adding shorter wavelength components along with longer wavelength components. The spectra are also very symmetric, but severely distorted by several modulation peaks. The amplitude filter

induced the lowest losses at the center frequency of 850 nm. The phase features a mainly quadratic shape over the mode-locked spectral range.

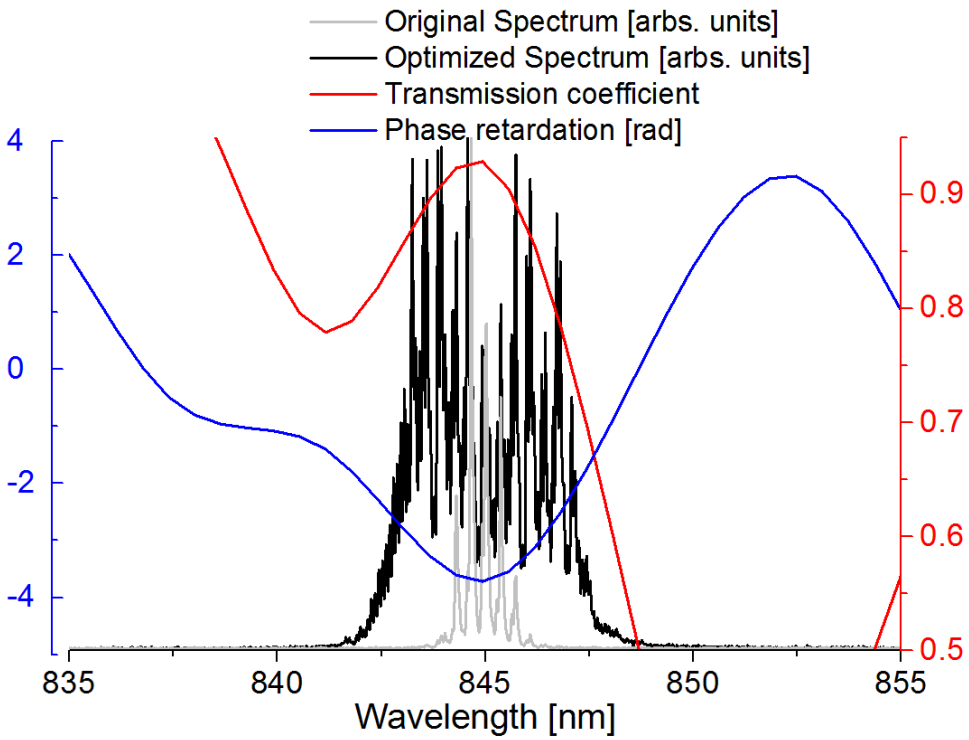

Fig. 9 shows the spectrum for active mode-locking before optimization (light grey) and after optimization (black). Additionally the amplitude filter (red) and the dispersion (blue) are shown.

After these initial investigations it was concluded, that the dispersion and spectral amplitude inside an edge-emitting semiconductor laser are of critical importance. The optical bandwidth could be increased for all mode-locking regimes. Though the results for active mode-locking were worse than for the other regimes, the spectral position of the emitted pulse strongly suggests, that the saturable absorber is suppressing shorter wavelength components in the other mode-locking regimes, namely passive and hybrid mode-locking. This means that on the one hand a correct spectral representation of the absorber is integral for a precise simulation of ultrafast edge-emitting semiconductor laser systems, and on the other hand, the absorption of the saturable absorber has to be tailored in order to achieve considerably better results.

To gain further insights on the relative influences of the dispersion and amplitude filters, the passive mode-locking regimes was examined closer. Passive mode-locking was chosen, because it featured a strong quadratic component in phase retardation, leading to a mostly linear chirp which was estimated to also lead to compressible optical pulses. In addition, the absence of a modulation current of this regime reduces the simulation effort later on significantly.

For closer inspection upon the impact of dispersion control and the amplitude filter, both were inspected separately. The setup was slightly different to the studies in Fig.7-9, so that the original output spectrum was already broader than before and the

evolutionary algorithm was expanded upon. The results for optimizing only the dispersion are depicted in Fig. 10 (left).

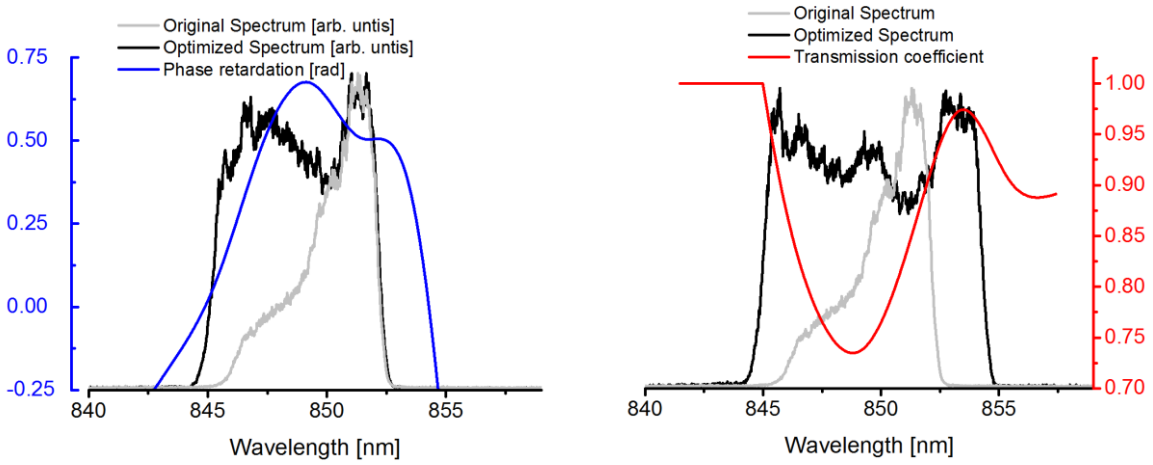

Fig. 10 Spectrum before optimization (light grey) and after optimization (black) for dispersion optimization (left, blue) and amplitude optimization (right, red).

The orientation of the phase retardation changed and the non-quadratic part of the phase orientation has shifted to longer wavelength. The spectral bandwidth only increased a bit by adding short wavelength components. The general shape of the amplitude filter (see Fig.10 right) however remains. The highest losses are applied to the middle of the spectrum at around 849 nm and decrease to the sides. For the amplitude optimization, lower wavelength components as well as higher wavelength components could be added, resulting in a spectral bandwidth of 10 nm, which is even higher than the optical bandwidth achieved earlier by hybrid mode-locking. Consequently, simultaneous dispersion and amplitude were now applied again to achieve the broadest possible spectrum. The results is depicted in Fig. 11.

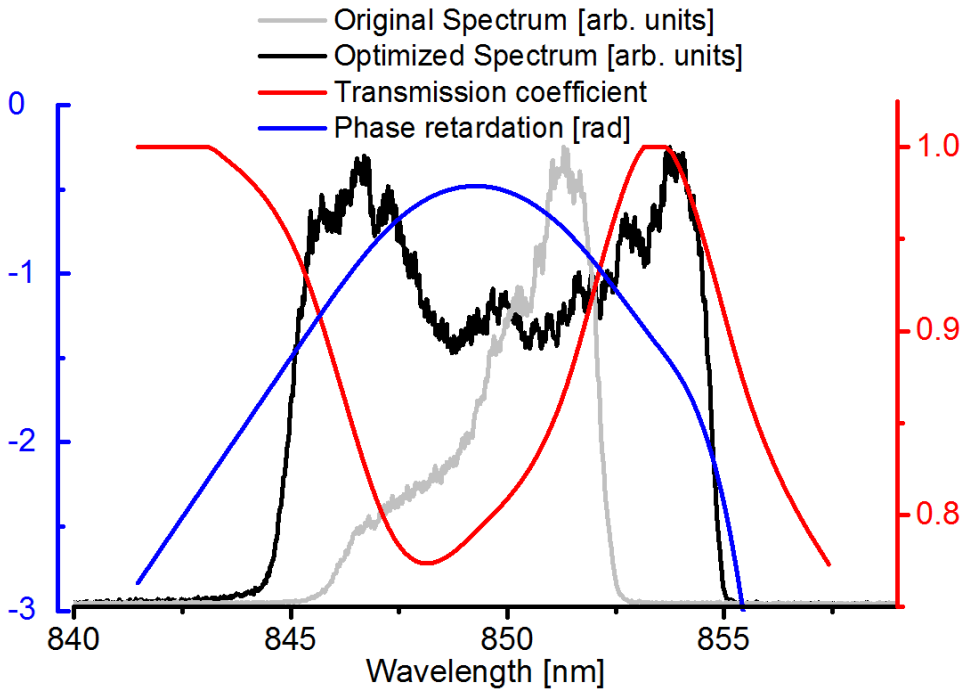

Fig. 11 Spectrum before optimization (light grey) and after optimization (black). Additionally the amplitude filter (red) and the dispersion (blue) are shown.

The introduced dispersion is larger than before and mostly quadratic over the complete spectrum. The shape of the amplitude filter is similar to before. The bandwidth was increased to 10.4 nm. But the increment to amplitude –only optimization is only 0.4 nm. To verify that the complete spectrum is mode-locked and to get a good estimation of the pulse width, the temporal pulse was compressed and the measured autocorrelation was compared with an autocorrelation trace calculated from the spectrum itself. The electrical spectrum of the laser system was measured as well. These data are depicted in Fig. 12.

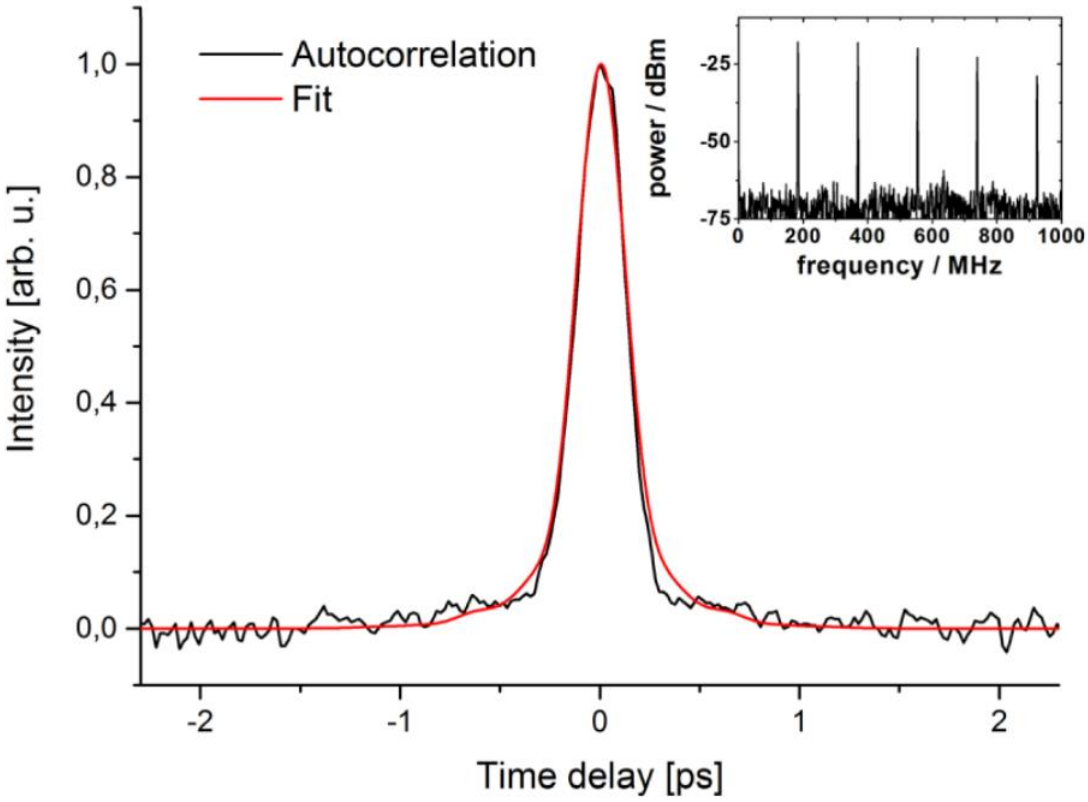

Fig. 12: Comparison between the measured autocorrelation (black) and the calculated autocorrelation (red). The electrical spectrum of the laser system is depicted as well.

Since the calculated and measured traces align well, a Fourier-limited record pulse width of 216 fs is estimated [12]. This verifies that dispersion and more crucial spectral amplitude filtering are a key strategy to generate ultrashort pulses with edge-emitting diode lasers. This supports the need of a precise understanding of the spectral gain and absorption dynamics of the active material and the related carrier dynamics for these devices.

To further investigate the dispersion and amplitude optimization of the laser system, the correlation between the net gain of the system and the optimized amplitude shape was analyzed. The results are depicted in Fig. 13.

For investigation of the spectral amplitude filter, we swept the operating wavelength of the laser system with the spatial light modulator. For each wavelength regime the threshold current was recorded as a measure of the net gain at this wavelength. The shape of the amplitude filter closely resembles the diagram of the threshold currents.

This strongly suggests, that the amplitude filter levels out the spectral net gain to produce a flat net gain for the laser system.

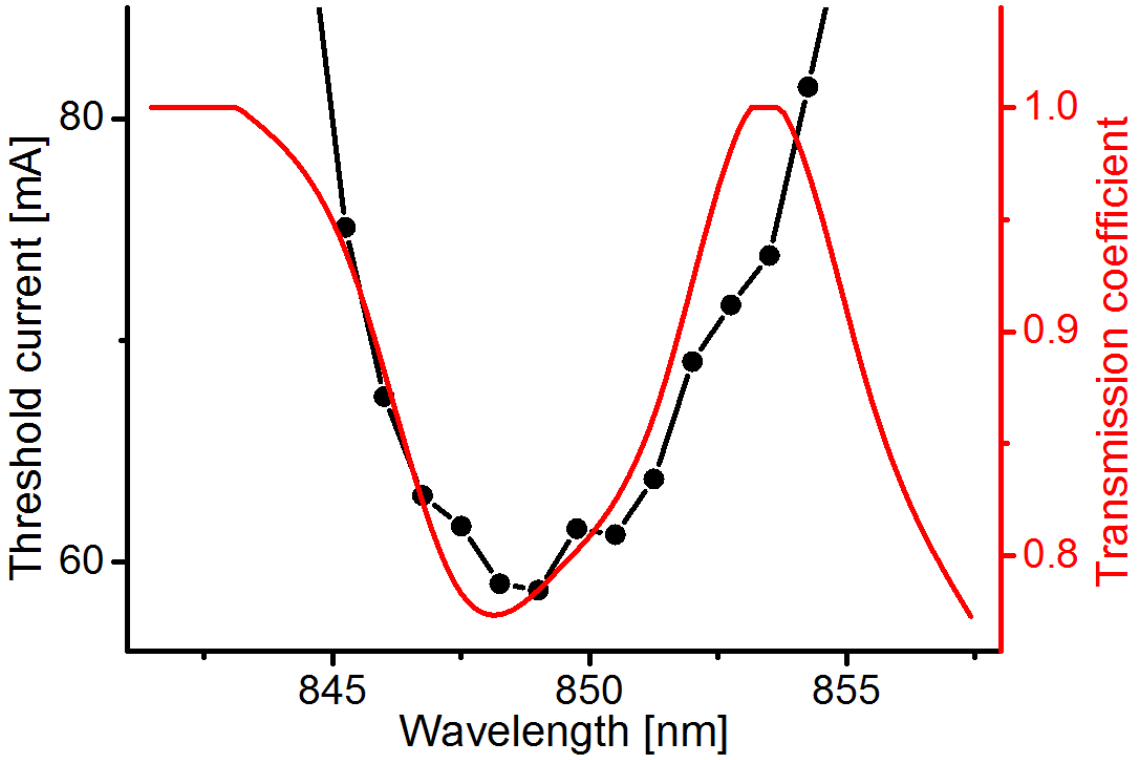

Fig. 13: The inversed quasi-net gain (black) is overlays with the optimal amplitude filter (red).

In summary, all three different mode-locking regimes were investigated. It was shown that dispersion and amplitude management is of importance to achieve broad spectral bandwidths for all regimes. It was displayed, that the saturable absorber prevents shorter wavelength components from lasing due to its spectral absorption, being unable to be saturated at these wavelengths. Because it was most accessible and best understood, passive mode-locking was chosen for closer analysis. It was shown that the amplitude filter has a major impact on the optical bandwidth of the tested system. A record pulse width of 216 fs was generated utilizing dispersion and amplitude optimization. It was shown, that the induced amplitude filters levels out the spectral net gain to create a flat net gain.

3. Conclusions and further strategy

In contrast to our initial plans, the implementation of a numerical model for a mode-locked diode laser that includes a microscopic modelling of the semiconductor susceptibility was not performed for two reasons: first, the original plan to implement the microscopic model into the Javaloyes model failed because of a numerical instability of the model. The alternative approach on the basis of the Haus model could be implemented but the calculations turned out to be extremely time consuming (17h for one simulation) but yet provided no clear evidence for many-body effects having a crucial influence at this stage. In contrast, our experimental investigations performed in parallel to the numerical analysis, clearly showed, that further progress towards

generation of shorter pulses is inhibited by a material related problem which is not determined by many-body effects in the first place: the steep absorption edge of the saturable absorber severely reduces the net gain spectrum and thus prevents the generation of sub-100fs pulses.

Thus, we elaborated a new semiconductor material structure together with our partners, the Ferdinand-Braun-Institute and the University of Arizona. This consists of chirped multiple quantum well diodes, which feature very broad and flat gain and absorption spectra.

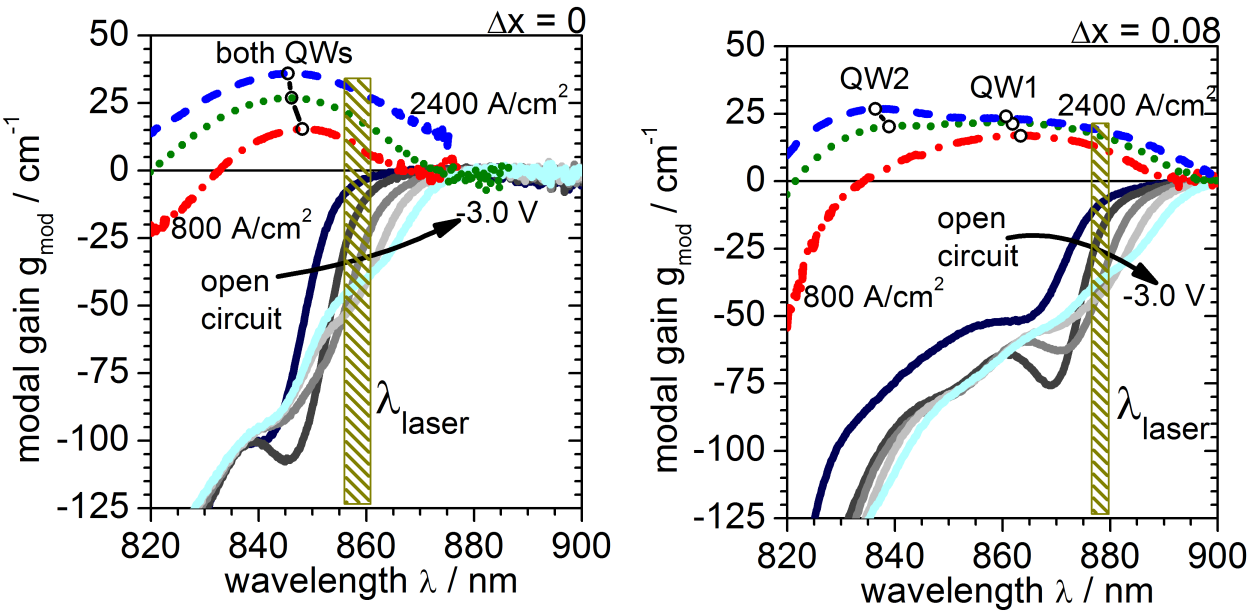

Fig.14 Left: Gain and absorption spectra for standard quantum wells. Right: gain and absorption spectra for chirped quantum wells

Figure 14 indicates the desired effect. The use of chirped quantum wells indicates that the quantum wells in the active region have slightly different compositions in order to broaden gain and absorption spectra. The left picture shows gain and absorption spectra for two identical quantum wells ($\Delta x=0$) which corresponds to the devices analyzed so far. The right graph shows absorption and gain spectra for two different quantum wells ($\Delta x=0.08$). It is obvious that the gain spectra broaden and the absorption edge of the absorber is now less steep at the short wavelength side. Such devices have already been produced and pre-characterized by the Ferdinand-Braun Institute. Recently, they have been antireflection coated and now they have been delivered to us after expiration of this project. Nevertheless, from the knowledge accumulated in this project, we expect, that a tremendous improvement of the shortest pulse width towards the 100 fs barrier becomes possible. After achievement of this milestone, we expect, that simulations containing a many-body semiconductor description will be an important tool for further optimization.

References (own publications linked to this project are marked with *):

1 “Multimode dynamics in bidirectional laser cavities by folding space into time delay”, J. Javaloyes and S. Balle, Opt. Express, Vol. 20, no. 8, pp. 8496–8502, 2012

2 “Freetwm: a simulation tool for multisection semiconductor lasers”, J. Javaloyes and S. Balle, 2012, Online

3 “Structures for additive pulse mode locking”, H. A. Haus *et al.*, J. Opt. Soc. Am. B 8 (10), 2068, 1991

4* “Femtosecond semiconductor laser system with resonator-internal dispersion adaptation”, Rouven H. Pilny, Benjamin Döpke, Jan C. Balzer, Carsten Brenner, Andreas Klehr, Andrea Knigge, Günther Tränkle, Martin R. Hofmann, Optics Letters, 42, Issue 8, pp. 1524-1527 (2017), doi: 10.1364/OL.42.001524

5* „Interaction of phase and amplitude shaping in an external cavity semiconductor laser“, Rouven H. Pilny, Benjamin Döpke, Jan C. Balzer, Carsten Brenner, Andreas Klehr, Götz Erbert, Günther Tränkle, Martin R. Hofmann, SPIE Photonics West, San Francisco, 2016

6* „Interaction of phase and amplitude shaping in an external cavity semiconductor laser“, Rouven H. Pilny, Benjamin Döpke, Jan C. Balzer, Carsten Brenner, Andreas Klehr, Götz Erbert, Günther Tränkle, Martin R. Hofmann, Proc. SPIE 9767; DOI: 10. 1117/12.2212906

7* „Impact of resonator-internal pulse shaping in mode-locked diode lasers”, Rouven H. Pilny, Benjamin Döpke, Carsten Brenner, Thomas Prziwarka, Andreas Klehr, Hans Wenzel, Andrea Knigge, Jörg Hader, Martin R. Hofmann, Nonlinear Dynamics in Semiconductor Lasers, WIAS Berlin, 2016

8* „Intracavity phase and amplitude shaping of a passively mode-locked semiconductor laser”, Rouven H. Pilny, Benjamin Döpke, Carsten Brenner, Martin R. Hofmann, Semiconductor and Integrated Optoelectronics, Cardiff, 2015

9* “Spectral broadening of mode-locked semiconductor lasers by resonator-internal pulse shaping”, Benjamin Döpke, Rouven H. Pilny, Carsten Brenner, Jan C. Balzer, Andreas Klehr, Götz Erbert, Günther Tränkle, Martin R. Hofmann, CLEO Europe, Munich, 2015

10* “Optimization of a mode-locked diode laser by manipulation of intracavity dispersion and absorption with an evolutionary algorithm”, Rouven H. Pilny, Benjamin Döpke, Carsten Brenner, Jan C. Balzer, Martin R. Hofmann, CLEO Europe, Munich, 2015

11* ”Ultrashort pulse generation with semiconductor lasers using intracavity phase- and amplitude pulse shaping”, Benjamin Döpke, Jan C. Balzer, Rouven H. Pilny, Carsten Brenner, Andreas Klehr, Götz Erbert, Günther Tränkle, Martin R. Hofmann, SPIE Photonics West, San Francisco, Proc. SPIE 9382-13, 2015

12* “Self-optimizing passively, actively and hybridly mode-locked diode lasers”, Rouven H. Pilny, Benjamin Döpke, Mohammad Ali Alloush, Carsten Brenner, A. Klehr, A. Knigge, G. Tränkle, Martin R. Hofmann, CB-P.2, CLEO/Europe 2017, Munich (2017)

13* “Ultrafast Diode Laser with Self-Adapting Pulse-Shaping in Passive, Active and Hybrid Mode-Locking Operation”, Rouven H. Pilny, Benjamin Döpke, Mohammad Ali Alloush, Carsten Brenner, Martin R. Hofmann, JTh2A.128, Optics + Photonics Conference, San Diego (2017)

14* “Impact of resonator-internal pulse shaping in mode-locked diode lasers”, Rouven H. Pilny, Benjamin Döpke, Carsten Brenner, Thomas Prziwarka, Andreas Klehr, Hans Wenzel, Andrea Knigge, Jörg Hader, Martin R. Hofmann, Nonlinear Dynamics in Semiconductor Lasers, WIAS Berlin (2016)

15* “Passive, active, and hybrid mode-locking in a self-optimized ultrafast diode laser”, M. Ali Alloush, Rouven H. Pilny, Carsten Brenner, Andreas Klehr, Andrea Knigge, Günther Tränkle, Martin R. Hofmann, SPIE Photonics West (OPTO), San Francisco (2018), Proc. SPIE 10553; DOI: 10.1117/12.2290086

16 „Fourier-Transform External Cavity lasers“, M. Breede, S. Hoffmann, J. Zimmermann, J. Struckmeier , M. Hofmann, T. Kleine-Ostmann, P. Knobloch, M. Koch, J.P. Meyn, M. Matus, S.W. Koch, and J.V. Moloney, Opt. Commun. 207, 261 (2002)